Performance of the Solar Simulator

Simulator beam characteristics were measured with the simulator completely assembled optically but not coupled to the chamber.

The results of simulator performance measurements are presented in Tables 1 and 2. Total intensity range was determined by a calibrated radiometer. Three to 10 lamps were used for the specified total intensity range. Lower or higher intensities than those specified in Table 1 can be obtained since one to 13 lamps can be operated. Rotational uniformity scans, at one-half and two solar constants (sc) were made at three locations along the length of the beam within the chamber test volume. Measurements, in incremental radii of 3 in., were made with a 4- by 4-cm array of solar cells. Collimation angle was determined from the geometrical relationship between the image source size and the distance between the image and the decollimation pinhole point.

A total of 11 spectral measurements were made, for both 0.5 sc and 2 sc, throughout the portion of the beam within the chamber test volume. (The measurements were taken at 11 locations within the beam. At each location the measurements were broken down in 14 bandwidths as noted in Fig. 2.) The range of deviation from the NRL (Naval Research Laboratory) solar distribution curve of the 11 measurements taken for each bandwidth and intensity level is listed in Table 2. The measurements were made by a double prism monochromator calibrated with a 1000-w NBS (National Bureau of Standards) Standard of Spectral Irradiance. A photomultiplier detector was employed for wavelengths from 0.25 to 0.65 μ and a lead sulfide detector for wavelengths from 0.45 to 2.7 μ. Radiation from both the standard lamp and solar simulator was diffused by a quartz transmissive diffuser prior to passing through the monochromator entrance slit.

A 24-hr continuous unattended operational test was performed on the system in which its ability to stabilize and automatically maintain a preset total intensity level was determined. Beam intensity stabilization and total intensity variations were measured by a solar cell whose output was recorded on a chart recorder.

Chamber Performance

Chamber tests were conducted immediately before and after modifications to determine to what degree chamber performance was affected by the addition of solar simulation. Tests were conducted with the facility operated in two different modes. In one, the inner chamber was cooled down to 88°K with no flow in the helium cryopanel. In the other, the helium cryopanel was cooled down to 5°K. Pressure measurements were made with a hot cathode ionization gage calibrated for nitorgen. For the first mode, the ultimate pressure increased from 4×10^{-10} torr to 3×10^{-9} torr due to chamber modifications for solar simulation. For the second mode, the ultimate pressure reached the ionization gage x-ray limit of 3×10^{-10} torr both before and after modifications.

Table 2 Spectral match

Bandwidth, μ	Deviation from NRL curve, %	
	2 s.c.	$\frac{1}{2}$ s.c.
0.25 to 0.33	−25.1 to 47.7	−12.1 to −51.8
0.33 to 0.40	9.0 to −10.2	20.4 to 3.0
0.40 to 0.50	0.7 to −11.0	5.4 to −1.9
0.50 to 0.60	1.8 to −2.3	6.1 to −0.3
0.60 to 0.70	−0.1 to −2.6	2.7 to −3.6
0.70 to 0.80	8.9 to −4.4	0.1 to −6.9
0.80 to 0.90	5.6 to −14.6	0.5 to −22.5
0.90 to 1.00	1.5 to −11.5	3.3 to −21.1
1.00 to 1.20	7.9 to 1.0	9.4 to −5.6
1.20 to 1.40	−11.3 to −17.0	−13.9 to −20.8
1.40 to 1.60	53.6 to 39.2	46.2 to 28.9
1.60 to 2.00	25.5 to 9.8	14.9 to −2.1
2.00 to 2.40	38.6 to −15.6	26.6 to −0.7
2.40 to 2.70	−12.4 to −30.9	15.5 to −43.0

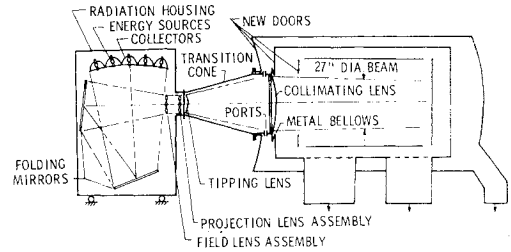

Fig. 2 Combined solar-vacuum facility.

References

[1] Elderkin, C. D. and Bradford, J. M., "A Large Ultra High Vacuum Environmental Chamber With Liquid Helium Cooled Walls," paper presented at 1965 Institute of Environmental Sciences Symposium, April 1965.

[2] Gregory, G. L., Bradford, J. M., and Mugler, J. P., Jr., "Vacuum Capabilities of the 150-Cubic-Foot Space Vacuum Facility at the Langley Research Center," *AIAA/IES/ASTM Space Simulation Conference*, AIAA, New York, 1966.

Radiation Interchange Interior to Multilayer Insulation Blankets

R. K. MacGregor,* J. T. Pogson,* and D. J. Russell†
The Boeing Company, Aerospace Systems Division, Seattle, Wash.

MULTILAYER insulation blankets provide a lightweight insulation system with a high thermal resistance. The multilayer blankets consist of a number of highly reflecting radiation shields interspaced with a low thermal conductivity spacer material or separated by crinkling the radiation shields themselves. The radiation shields are generally mylar or kapton films metalized on one or both sides. Spacer materials range from very coarse silk or nylon net to continuous materials such as a borosilicate fiber glass paper.‡ While heat transfer through the insulation normal to the layers is small, there are large energy losses at seams and

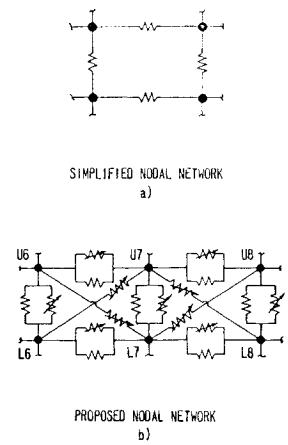

Fig. 1 Nodal networks utilized for multilayer insulation calculations.

Received October 20, 1969.
* Research Specialist. Member AIAA.
† Research Engineer
‡ Tissue glass.

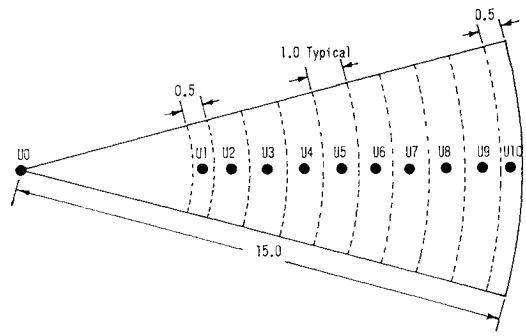

Fig. 2 Sectioned plan view of multilayer insulation blanket.

penetrations in the blanket which are enhanced by its anisotropic nature. Conductance along the layers of the blanket may be two to three orders of magnitude greater than transport normal to the layers. Thus, the energy loss at discontinuities in the blanket affects temperature distributions over substantial regions of the blanket.
the layers, and temperature distributions over substantial regions of the blanket may be affected.

Investigators utilizing nodal models[1,2] for the determination of multidimensional heat transfer interior to multilayer blankets have employed simplified networks. These nodal networks (Fig. la) have generally combined the conduction and radiation transport into a single term and have required experimentally measured conductance values for these connectors along the layers. In this study, a more detailed network (Fig. 1b) permits the radiation and conduction transport along and between the layers to be treated separately. The radiant energy exchange is determined by computing radiation interchange factors based on Seban's specular-diffuse reflectance model.[3] The interchange factors are calculated by a Monte-Carlo computer program.[4,5] Inputs to the program are the blanket geometry and basic material radiative properties (i.e., emissivity, specular reflectance and total reflectance).

The geometry studied was a 30-in.-diam blanket (Fig. 2) with a spacing between radiation shields set at 0.02 in. (50 layers/in.). A single geometric configuration with four different material combinations was considered. These hypothetical blankets were constructed of 1) single aluminized mylar with a noninteracting spacer; 2) double aluminized mylar with a noninteracting spacer; and 3) double aluminized mylar with a tissue glass spacer. The calculations were completed twice for the double aluminized mylar with the noninteracting spacer; once using a specular-diffuse reflectance model and once with a totally diffuse reflectance. The radiative properties of the materials are listed in Table 1.

Table 1 Measured material radiative properties

Property[a]	Aluminum	Diffuse aluminum	Mylar	Tissue glass
ϵ	0.030	0.030	0.273	0.0[b]
ρ^d	0.024	0.970	0.065	0.330
ρ^s	0.946	0.0	0.662	0.0
τ^d	0.0	0.0	0.0	0.670

[a] ϵ emissivity, ρ^d diffuse reflectance, ρ^s specular reflectance, τ^d diffused transmittance.
[b] Tissue glass assumed to be at equilibrium; all energy absorbed is reemitted; transmission and reflection increased to account for effective reemission.

Discussion of Results

The normalized radiation interchange factors ($\mathfrak{F}_{ij}/\epsilon_i$) between a series of nodes on two adjacent radiation shields within a multilayer insulation blanket have been calculated. The factors shown are for a single typical node (L7 on the lower radiation shield) to all other nodes in the system, rather than the matrix of exchange factors which would be required to determine the over-all temperature distribution. The results of these calculations are shown in Table 2.

Where L7 is the emitting node, the factors to L6 and L8 indicate radiant transfer which augments conduction along the individual layers. The factor to U7 indicates the normal radiant transfer between the layers, while the factors to U6 and U8 indicate "diagonal" transfer between the layers.

For the double aluminized mylar blanket with a specular-diffuse reflectance model and a noninteracting spacer, one observes that

Table 2 Normalized radiation interchange factors (emitter node L7)

			Double aluminized mylar		
Node	Node area, in.^{2}	Single aluminized mylar specular-diffuse reflectance noninteracting spacer	Specular-diffuse reflectance noninteracting spacer	Diffuse reflectance noninteracting spacer	Specular-diffuse reflectance tissue glass spacer
L0	113.10	0.0	0.00031	0.0	0.0
L1	19.63	0.0	0.00018	0.0	0.0
L2	43.98	0.0	0.00049	0.0	0.0
L3	50.27	0.0	0.00112	0.0	0.0
L4	56.54	0.00003	0.00321	0.00010	0.00004
L5	62.84	0.00010	0.00979	0.00028	0.00009
L6	69.12	0.00377	0.06246	0.03288	0.02677
L7	75.39	0.06543	0.32780	0.42347	0.44226
L8	81.69	0.00413	0.06741	0.03348	0.02549
L9	87.97	0.00023	0.01018	0.00087	0.00060
L10	46.33	0.00003	0.00167	0.00018	0.0
Subtotal		0.07372	0.48462	0.49140	0.49534
U0	113.10	0.0	0.00031	0.0	0.0
U1	19.63	0.0	0.00021	0.0	0.0
U2	43.98	0.00003	0.00049	0.0	0.0
U3	50.27	0.00010	0.00112	0.0	0.0
U4	56.54	0.00020	0.00317	0.00011	0.0
U5	62.84	0.00170	0.00993	0.00028	0.00013
U6	69.12	0.03997	0.06256	0.03316	0.02638
U7	75.39	0.83463	0.34376	0.43965	0.45117
U8	81.69	0.04627	0.06776	0.03372	0.02672
U9	87.97	0.00207	0.01021	0.00087	0.00055
U10	46.33	0.00050	0.00178	0.00018	0.0
Subtotal		0.92551	0.5013	0.50811	0.50398

1) Over 6% of the energy emitted from node L7 is transferred along that layer to node L8. This small radiative transfer increment, even in regions where the temperature gradient along the layer is small, may significantly augment if not overwhelm the conduction transfer along the layer.

2) Over one-third of the emitted energy is transferred to the facing node U7, and 6% is transferred to node U8. This cross-radiation transfer may again overpower conduction along the facing layer, particularly when combined with a similar radiative transport from node U7.

Several investigators[6,7] have experimentally evaluated the effective thermal conductance along the layers of multilayer insulation and have shown substantial increases over that conductance due to the layer material itself. This experimental data, which is strongly temperature dependent, is then utilized in nodal network models to calculate thermal performance.

The addition of radiator connectors to the nodal network both along individual layers and as cross connections between layers may eliminate the need for experimental effective conductance studies along the layers to supplement analytic solutions.

A comparison of single and double aluminized insulation systems indicates the performance advantages of double aluminizing over single for the case of the noninteracting spacer. Conduction between the layers tends to reduce the magnitude of this effect.

A comparison of the results for double aluminized mylar using the specular-diffuse model, as opposed to an only diffuse reflectance model, shows that significant errors will result with the latter—the normal heat transfer is overestimated and the parallel radiative transport is underestimated. Thus, a capability for handling the specular component of reflection is necessary to treat numerically the radiation transfer interior to multilayer insulation blankets.

The net effect of a tissue glass spacer is to diffuse the energy being reflected between the layers. A comparison of the double aluminized cases with a tissue glass spacer (specular-diffuse reflection) and with a noninteracting spacer (diffuse reflection) shows good agreement between the two results.

Summary

In summary, a study of the radiation interchange factors between nodes on adjacent layers of a multilayer insulation blanket has shown that 1) radiative transport along both layers is a significant mode of energy transport; 2) specular-diffuse reflectance models are necessary for the calculation of radiant interchange factors in the case of noninteracting spacers; 3) diffuse reflectance models allow a good approximation to the results for blankets utilizing continuous diffusing spacers such as tissue glass.

References

[1] Cunnington, G. R. et al., "Performance of Multilayer Insulation Systems for Temperatures to 700°K," CR-907, Oct. 1967, NASA.

[2] Johnson, W. R. and Sprague, E. L., "Analytical Investigation of Thermal Degradation of High-Performance Multilayer Insulation in the Vicinity of a Penetration," TN D-4778, Sept. 1968, NASA.

[3] Seban, R. A., "Discussion of an Enclosure Theory of Radiative Exchange Between Specularly and Diffusely Reflecting Surfaces," *Transactions of the ASME, Ser. C: Journal of Heat Transfer*, Vol. 84, 1962, pp. 299–300.

[4] Corlett, R. C., "Direct Monte-Carlo Calculation of Thermal Radiation in Vacuum," *Transactions of the ASME, Ser. C: Journal of Heat Transfer*, Vol. 88, 1966, pp. 376–382.

[5] Drake, R. L., Lester, A. B., and MacGregor, R. K., "Thermal Radiative Interchange Factor Program," Document D2-114470-1, Jan. 1969, The Boeing Co.

[6] Caren, R. P. and Cunnington, G. R., "Heat Transfer in Multilayer Insulation Systems," *Advances in Cryogenic Heat Transfer*, Chemical Engineers Progress Symposium Series, Vol. 64, No. 87, 1968.

[7] Androulakis, J. G. and Kosson, R. L., "Effective Thermal Conductivity Parallel to the Laminations and Total Conductance of Multilayer Insulation," *Journal of Spacecraft and Rockets*, Vol. 6, No. 7, July 1969, pp. 841–845.